SPE-191424-18IHFT-MS

Polyelectrolyte Complex Stabilized CO_2 Foam Systems for Improved Fracture Conductivity and Reduced Fluid Loss

Rudhra Anandan, Reza Barati, and Stephen Johnson, The University of Kansas

This paper was prepared for presentation at the SPE International Hydraulic Fracturing Technology Conference and Exhibition held in Muscat, Oman, 16 - 18 October 2018.

Abstract

The objective of this work was to develop a supercritical CO_2 foam with a liquid phase composed of a polyelectrolyte complex nanoparticle system interacting with a viscoelastic surfactant solution. This is intended to be used as a fracturing fluid to reduce fluid loss and increase post-fracture clean-up efficiency for improved productivity in unconventional reservoirs. In a previous study, we optimized the polycation/polyanion ratio and polyelectrolyte pH using zeta potential and phase-angle light scattering. Rheological and foam stability tests were used to further optimize surfactant/polyelectrolyte ratio. In this work, dynamic fluid loss tests were performed on supercritical CO_2 foam generated using the optimized ratio of surfactant/PECNP to investigate the effect of PECNP addition to the surfactant solution on the fluid loss. The same foam systems were used to investigate post fracture clean up using sand pack tests. Interfacial tension was measured on both air-(surfactant/PECNP) and supercritical CO_2-(surfactant/PECNP) systems to understand the effect of PECNP on IFT. Fluid loss to the formation during hydraulic fracturing causes water blockage, formation damage and capillary pressure shift, lowering the conductivity of the reservoir, and impeding the flow of oil and gas. Supercritical CO_2 foam generated by surfactant solution exhibited low fluid loss, thus lower values of fluid loss coefficient compared to unfoamed surfactant systems. However, addition of polyelectrolyte complex nanoparticles further reduced the total fluid loss and fluid loss coefficient. Foam fracturing fluids break in the presence of crude oil because the oil penetrates the foam lamellae causing drainage and lamellar rupture; this results in effective post fracture clean up using supercritical CO_2 foam as fracturing fluid. Foam systems generated by surfactant showed promising clean up results, and the addition of PECNP further increased clean up efficiency. From IFT test results we concluded that the addition of PECNP decreased interfacial tension of both air-(surfactant/PECNP) and supercritical CO_2-(surfactant/PECNP) systems. The addition of optimized polyelectrolyte complex nanoparticles to surfactant in a supercritical CO_2 foam fracturing fluid can reduce interfacial tension and fluid loss, which will reduce formation damage, resulting in better hydrocarbon flow. PECNP stabilized surfactant-supercritical CO_2 foam drains rapidly in the presence of crude oil, leading to good clean-up, which will result in better flow back and higher productivity.

Introduction and Literature Review

Hydraulic fracturing is a stimulation technique to enhance production of hydrocarbons in a target geologic formation by injecting fracturing fluid under pressures greater than parting pressure of the rock to fracture the formation (Economides and Nolte, 2000; Kohshour et al, 2016). Starting from the first hydraulic fracturing job conducted in the Hugoton gas field of Kansas in 1947 [1] and subsequent commercial success in the US in Green River Basin, Piceance Basin [2], San Juan Basin and the Denver Basin (Fast et al, 1977), resulted in quick spread of the process into the rest of the US, Western Canada and North Sea [3]. The conjunction of techniques such as directional drilling, high volume fracturing and micro-seismic monitoring with the development of multi-well pads and multi stage fractures made production of hydrocarbon from shales and other unconventional reservoirs technically and economically feasible. However, hydraulic fracturing is a water-intensive process, the Environmental Protection Agency estimates that 70 to 140 billion gallons of water might be used annually for fracturing in the US [4].

Crucial stages involved in hydraulic fracturing include fracture design, preparation and pumping of fracturing fluid into the well resulting in fracture propagation; the final stage is flow back and production [5]. Fracturing fluids are essential components of the fracturing process. Their main purpose is to create networks of fractures from the wellbore extending into the formation and to suspend and transport proppants to the fractures in the formation to sustain the conductivity of the fracture for subsequent production of hydrocarbon [6]. Selection of proper fracturing fluid has a direct impact on the production of hydrocarbon. It must have sufficient viscosity to carry proppant, create sufficient fracture width, limit fluid loss, should not damage the fracture conductivity during flow back, should result in good clean up, and should be both environmentally benign and cost effective (Montgomery, 2013; Samuel et al, 1999). Slickwater is one of the most commonly used fracturing fluid, as the fluid is less viscous, damage to fracture conductivity is less (Barati and Liang, 2014), but, 30 to 90% of injected water can remain in the formation, which leads to capillary pressure discontinuity caused by formation damage, negatively affecting the flowback and hydrocarbon recovery (Sharma and Agrawal, 2013; Penny et al, 2006; Makhanov et al, 2012; Economides and Nolte, 2000). Viscous fracturing fluid such as cross-linked gels might damage the permeability of proppant pack and fracture conductivity resulting in reduction in hydrocarbon recovery (Barati et al, 2009; Barati and Liang, 2014).

Alternatives to water based fracturing fluids such as foams address the shortcomings of slickwater and cross-linked polymers. Foams and other energized fluids can transport proppants much more effectively than slick water (Economides and Nolte, 2000; Reidenbach et al, 1986), improve clean-up efficiency, lower fluid loss, reduce pressure drop due to friction, minimize formation damage, drastically reduce water usage and flow back water treatment (Blauer and Kohlhaas, 1974; Cawiezel and Niles, 1987). CO_2 foam has been as a fracturing fluid since the 1980s in South Texas (Friehauf and Sharma, 2009). CO_2 is an abundant and nonflammble gas;, CO_2 foam as fracturing fluid can achieve significant improvement in hydrocarbon recovery and reduction in completions cost compared to water based fracturing fluids (Burke and Nevison, 2011; Friehauf and Sharma, 2009; Yost, 1994; Linde, 2013).

Foam is a colloidal dispersion with liquid as the continuous phase and gas as the discontinous phase. In addition to protecting the gas/liquid interface to prevent coalescence, viscoelastic surfactant (VES) offers effective viscous behavior under stress to CO_2 foam which helps in fracture formation (Schramm, 1994; Barati and Liang, 2014). Adding nanoparticles to surfactant generated foam increases the adhesion energy at the interface resulting in a longer lasting foam (Yu et al., 2012) and improves the thermal stability and elasticity through structural condensation (Yang et al., 2017). Also, addition of polyelectrolytes further stabilizes the foam due to electrostatic and entropic interactions (Klitzing et al., 1997) that results in stable lamellae (Anandan et al., 2017; Veisi et al., 2018) and reduces the adsorption of surfactants on proppants (He et al., 2015).

Foams destabilize and breaks in the presence of crude oil (Schramm, 1994), because imbibition of oil into the foam lamellae causes them to rupture (Talebian et al., 2013), which results in breaking of foam, this in turn will increase the post fracture clean up efficiency.

In a previous study (Anandan et al., 2017), optimized pH of polyethylenimine and optimized mass ratio of polyethylenimine to dextran sulfate was determined based on minimizing particle size and maximizing absolute zeta potential. PECNP stabilized $scCO_2$ foam was subjected through rheology and foam stability tests, based on which an optimized surfactant- PECNP ratio was found. The objective of this work is to improve the performance of $scCO_2$ foam systems prepared using optimized surfactant-PECNP formulations through controlling the fluid loss and improving the post fracture clean up. Dynamic fluid loss and sand pack tests were performed to study and analyze the fluid loss and fracture clean up respectively.

Materials

Surfactant

The viscoelastic surfactant (Harcos Chemicals Inc, Kansas City, Kansas, USA. SDS# RD00364) used was an aqueous solution of a proprietary amphoteric surfactant designated HDP 0761-12-2AM. We will refer to it as "2AM" in this paper. It has a density of 1.0688 g/ml at 25°C.

Polyethylenimine

The polyethylenimine (PEI) used in this work is a branched polycation composed of amine groups and two-carbon aliphatic CH_2CH_2 spacer as the repeating groups. It contains primary, secondary and tertiary amino groups in the approximate ratio of 1:2:1 (Figure 1). PEI is a liquid with a density of 1.03 g/ml at 25°C, viscosity is between 1.3×10^4-1.8×10^4 cP at 50°C and an average molecular weight of 25,000 $g.mol^{-1}$. It was purchased from Sigma Aldrich, St Louis, Missouri, USA. (CAS# 9002-98-6).

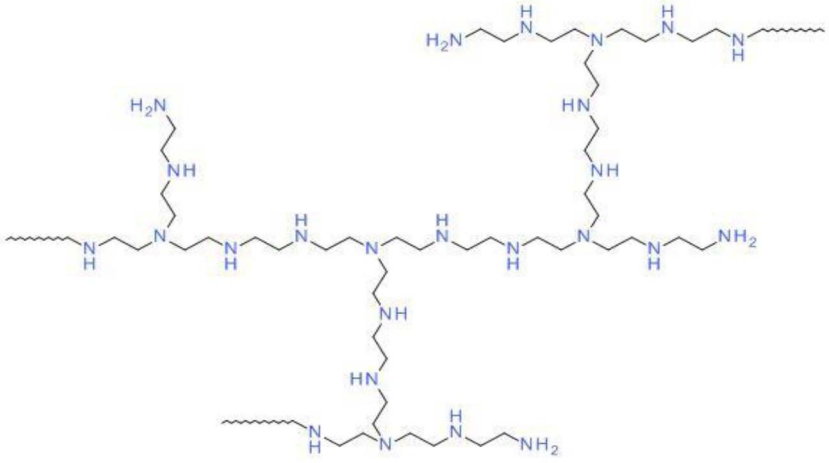

Figure 1—Chemical structure of branched PEI (Anandan et al., 2017)

Dextran Sulfate

Dextran sulfate (DS, Sigma Aldrich, St. Louis, Missouri, USA. CAS# 9011-18-1) is a polyanion with an average molecular weight of 500,000 $g.mol^{-1}$. Figure 2 shows the chemical structure of DS.

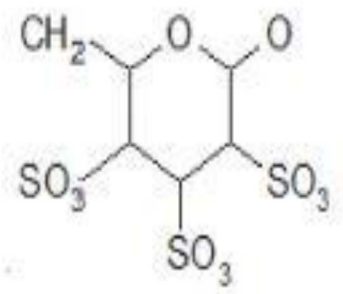

Figure 2—Chemical Structure of Dextran Sulphate Monomer [7]

Brine

Deionized water was used to prepare 2 wt% sodium chloride (NaCl). NaCl was purchased from Fisher Chemical, New Jersey, USA (CAS# 7647-14-5, ACS certified).

Crude Oil

Mississippian limestone play (MLP) crude oil with a density and viscosity of 0.82 $g.ml^{-1}$ and 3.88 cP, respectively at 40°C was used in the sand pack tests to study the fracture cleanup process.

Hydrochloric Acid

12N HCl (Fisher Chemical, New Jersey, USA. CAS # 7647-01-0, ACS certified) was used to adjust the pH of PEI solution to prepare the polyelectrolyte complex nanoparticle.

Cores

Kentucky tight sandstone outcrop core was used for the dynamic fluid loss experiment. Core plug was 0.88 in. diameter and 0.99 in long. The porosity and permeability of the core were 12.91 % and 0.11 mD, respectively.

Proppants

Ceramic proppant designated as CARBO EconoProp of 20/40 mesh size was used for the sand pack test. The proppant was provided by CARBO Ceramics.

Methods and Procedures

Sample Preparation

Polyethylenimine Solution. 1 wt% PEI solution was prepared using 2 wt% NaCl brine, stirred at 600 rpm for 60 minutes. The average initial pH of PEI solution was 11.2. PEI solution of pH 8.5 was prepared by addition of 12N HCl solution. As pH of 8.5 gave the most optimized nanoparticles based on the particle size and zeta potential measurements (Anandan et al., 2017), all the tests were performed using PEI solution adjusted to pH 8.5.

Dextran Sulphate Solution. The solution of 1 wt% DS solution was prepared using 2 wt% NaCl brine and it was stirred at 600 rpm for 60 minutes.

Surfactant Solution. The surfactant (2AM) solution was prepared in 2 wt% NaCl brine. The solution was stirred at 600 rpm for 20 minutes and the final concentration of the 2AM in all the solutions was kept at 1 wt%.

Polyelectrolyte Complex Nanoparticles (PECNP). Based on the particle size and zeta potential measurements (Anandan et al., 2017), 3:1:0.1 ratio of PEI: DS: 2wt% NaCl with pH of 8.5 for 1wt% PEI

showed the most desirable properties. Therefore, for all the tests, PECNP was prepared in the ratio of 3:1:0.1 of PEI (1wt%, pH 8.5): DS (1wt %): 2% NaCl and was stirred at 600 rpm for 20 minutes.

Surfactant-PECNP Solution. Surfactant solution of 1.67 wt%, 1.43 wt%, 1.25 wt% and 1.11 wt% were prepared and mixed with PECNP solution at 600 rpm for 20 minutes to prepare solutions of 2AM: PECNP wt ratios of 6:4, 7:3, 8:2, and 9:1 respectively. The final concentration of surfactant in the 2AM: PECNP solutions was 1 wt%.

Foam Quality. Foam quality refers to volumetric gas content, i.e. gas volume divided by foam volume at a given temperature and pressure. Supercritical CO_2 foams of quality 70%, 80%, 90% and 95% were used to perform the dynamic fluid loss tests and sand pack tests. For all four foam qualities the total foam flow rate was maintained at 6 ml/min. For example, to generate 90% foam quality, the CO_2 pump was operated at a flow rate of 5.4 ml/min and the aqueous solution pump was operated at a flow rate to 0.6 ml/min, which resulted in a total flow rate of 6ml/min.

Experimental Procedure

Interfacial Tension Measurements

The pendant drop method was used to measure air-aqueous phase and supercritical CO_2-aqueous phase interfacial tension. The chamber and lines were thoroughly rinsed with RO water and the main chamber was filled with the desired aqeous phase solution and the chamber was heated to 40°C. After increasing the chamber pressure to 1300 psi, a $scCO_2$ bubble was generated in the liquid chamber. A high-resolution camera was used to acquire the images of the drop and DROPimage software was employed to measure the interfacial tension. Figure 3 shows the schematic flow diagram of the IFT setup.

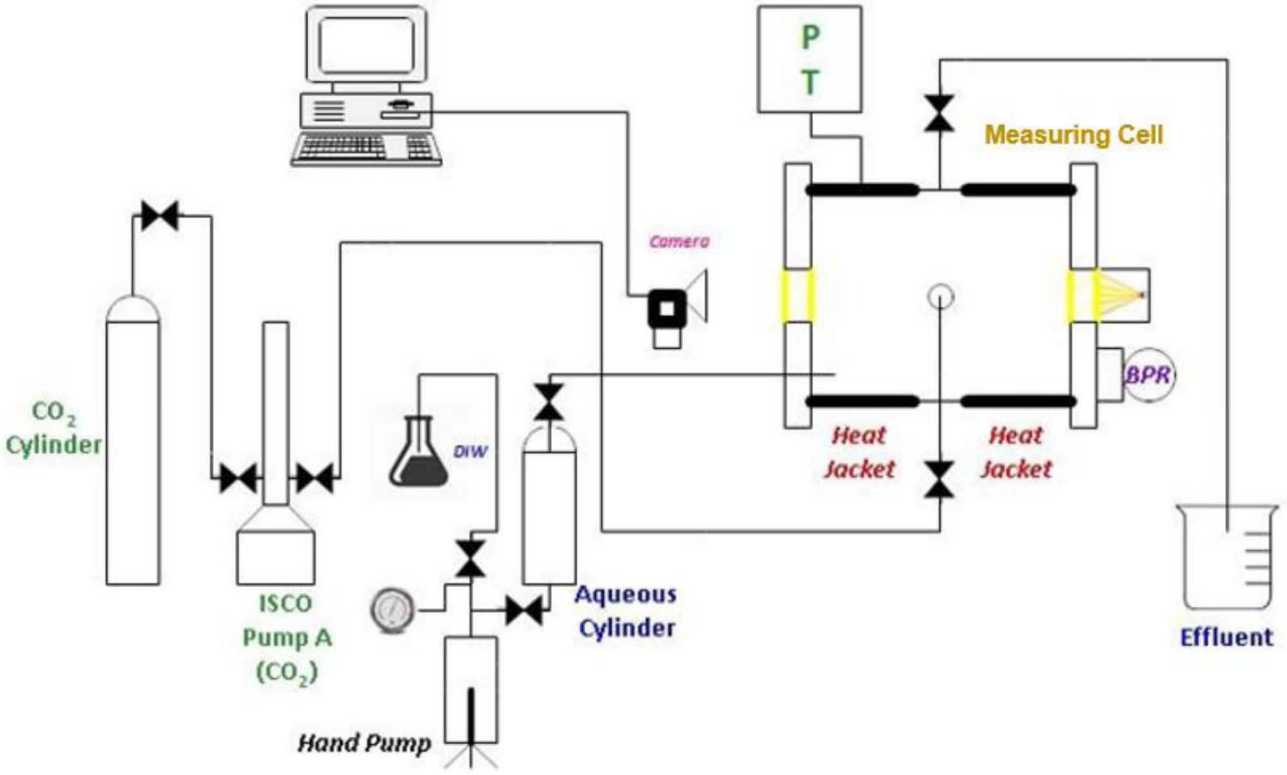

Figure 3—Schematic flow diagram of the IFT set up (Drawn by Negar Nazari, used by permission [8])

Porosity Measurement for Fluid Loss Experiment

The dimesnsions and dry weight of the Kentucky core were measured. Then the core was saturated in a vacuum desiccator using 2% NaCl brine and was weighed to get the saturated weight. Porosity was calculated using Equation 1 to Equation 3

$$V_b\ (cm^3) = \pi * r^2 * h \quad \text{Equation 1}$$

where, V_b is the bulk volume (cm^3), r is the radius of the core (cm) and h is the height of the core (cm)

$$V_p\ (cm^3) = (W_{sat} - W_{dry}) / \rho_{brine} \quad \text{Equation 2}$$

where,

V_p is the pore volume (cm^3), W_{sat} is the saturated weight of the core (cm^3), W_{dry} is the dry weight of the core (cm^3) and ρ_{brine} is the density of brine (g/cm^3)

$$\Phi\ (\%) = (V_p/V_b) * 100 \quad \text{Equation 3}$$

where,

Φ is the porosity

Permeability Measurement for Fluid Loss Experiment

Brine flooding experiments were performed to measure the core permeability. Figure 4 shows the schematic flow diagram of the core flooding setup. All the lines leading to the pressure transducer, pump A and pump B were filled with Soltrol. Accumulator A was filled with brine manually. Accumulators B and C were not used for this experiment. The accumulator has a piston, above the piston it was filled with brine (2% NaCl) and below the piston it was filled with Soltrol. Pump A was used to pump Soltrol which in turn will pump the brine out of the accumulator. All the flow lines leading to the core holder were filled with brine. Lines just before and after the core holder were filled with brine manually using syringe. Then the core was placed in the core holder and confining pressure or overburden pressure was applied using hydraulic oil. Flow was initiated into the core holder with 3 different flow rates and corresponding differential pressure was noted for different flow rates. These pressure drop vs flow rate readings were used to calculate the permeability using the Darcy's law:

$$Q = (k * A * (\Delta P)) / (\mu * L) \quad \text{Equation 4}$$

where,

k is permeability (mD), A is area (cm^2), ΔP is differential pressure (psi), μ is viscosity (cP), L is length of the core (cm) and Q is flow rate (ml/min).

After acquiring the readings, pump was stopped, the core holder was disconnected from the lines and Accumulator A was filled with RO water. This procedure was repeated to clean the lines with RO water.

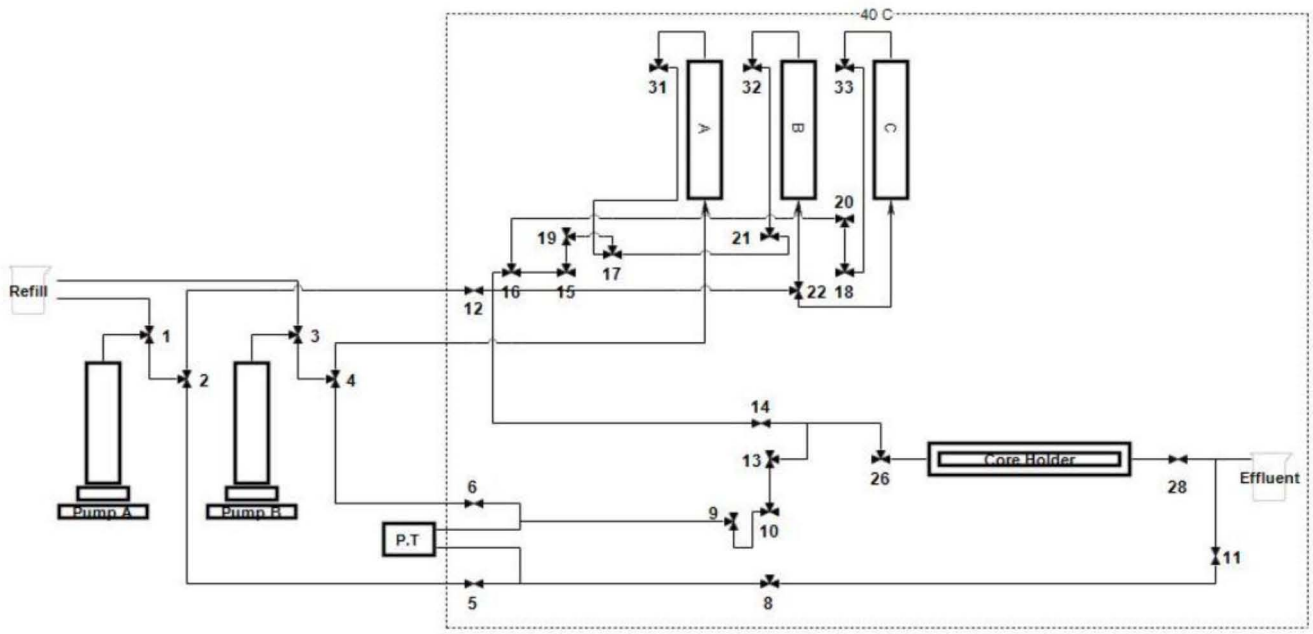

Figure 4—Schematic flow diagram of the core flood setup

Dynamic Fluid Loss Experiment

This was performed to measure the fluid loss from the fracturing fluid under the given pressure and temperature. The experiment was performed at 1300 psi and 40°C. As 8:2 ratio of 2AM: PECNP was the most optimized system (Anandan et al., 2017), CO_2 foam generated by it was used to perform fluid loss experiment at foam qualities of 70%, 80%, 90% and 95%. Its results were compared with CO_2 foam generated by the surfactant solution alone (1% 2AM). Real gas equation shown in Equation 5 below was used to convert the volume of $scCO_2$ measured by Alicat at room temperature and atmospheric pressure to volume at pressure and temperature of the test and Z factor of 0.51 [9] was used. Summation of the gaseous phase (CO_2) and aqueous phase fluid loss gave the total fluid loss. This value was used to calculate the fluid loss coefficient using the Carter leakoff equation shown in Equation 6.

$$PV = ZnRT \quad \text{Equation 5}$$

where,

P is pressure (psia), V is volume (cm^3), T is temperature (°C), n is number of moles, R is ideal gas constant

$$V_L = C_w * t^{(1/2)} + V_s \quad \text{Equation 6}$$

where,

V_L is total fluid loss (cm^3), C_w fluid loss coefficient, T is time (min) and V_s is spurt fluid loss (cm^3)

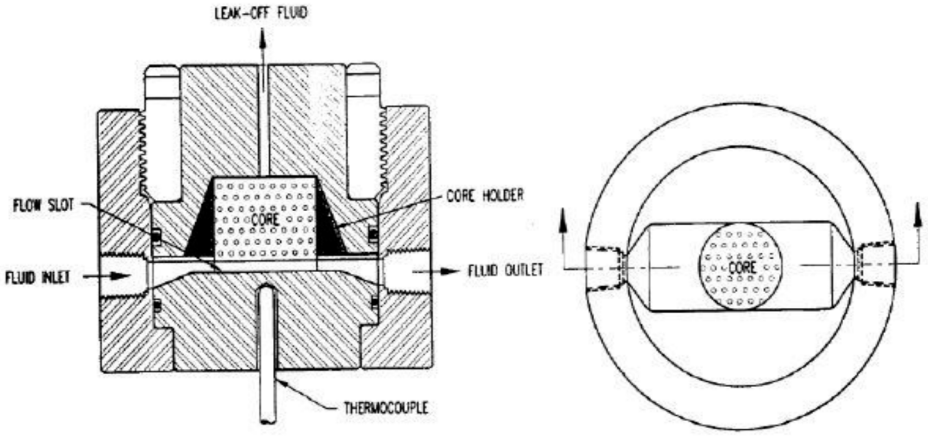

Figure 5—Schematic diagram of fluid loss cell [7]

As shown in Figure 5, the dynamic fluid loss cell contains one inlet and two outlets, one outlet for the fluid loss and other for the main effulent fluid, both outlets are connected to two different back pressure regulators. Nitrogen supplied from a cylinder is used to apply pressure to the back-pressure regulator. The inlets and outlets of the cell are made of quick-connect fittings. Leakage is prevented by O-ring seals plus a rubber core holder prevent fluid from bypassing the core.

Three ISCO pumps were needed to run this test. Pumps A & B act together as one single pump to inject the liquid and Pump C is used to deliver $scCO_2$. Accumulators and Pump C were refilled with liquid (2AM or 2AM-PECNP) and CO_2, respectively. Temperature and pressure of 40°C and 1300 psi, respectively, were set and the fluid loss line was kept at 50 psi less than the main effluent line of the fluid loss cell. Flow rates of Pumps A & B and Pump C were set based on the foam quality needed to run the experiment and pumps were turned on. Foam was generated using an inline mixer. Figure 6 shows the schematic flow diagram of the fluid loss experiment. After foam had passed through the fluid loss line, there was effluent both in fluid loss side as well as the main line of the fluid loss cell. The gaseous phase volume of the fluid from the fluid loss line was analyzed for CO_2 using an Alicat gas analyzer and aqueous phase from the fluid loss line is collected in a burette and volume collected vs time was noted.

Fracture Cleanup

Post-fracture cleanup or flow back of fracturing fluid is an important parameter which affects production. The fracture clean-up experiment was performed using a cyclindrical sand pack holder loaded with proppant. As the fluid system with 8:2 ratio of 2AM: PECNP was the most optimized system (Anandan et al., 2017), CO_2 foam generated by it was used to perform sand pack experiments at foam qualities of 70%, 80%, 90% and 95%. Its results were compared with CO_2 foam generated just by the surfactant solution (1% 2AM). Pore volume of the sand pack was measured by mass balance from dry and saturated weights. Before pore volume measurement, the sand pack holder dimensions were measured. Then the sand pack was loaded with ceramic proppant of 20/40 mesh size and weight of the sand pack loaded with proppant was measured. Dry weight of sand pack loaded with proppant and weight after saturation was measured. The difference in weight was the weight of brine in the sand pack. Equation 2 was used to find the pore volume.

After pore volume measurements, sand pack loaded with proppant was installed in the foam setup. Experimental setup was pressurized to 1300 psi and heated to 40°C. Then the brine flood was performed at a flow rate of 6, 10 and 12 ml/min and corresponding differential pressure across the sand pack was recorded using Lab View software. After brine flood, a foam flood was performed, and foam of desired quality was generated by adjusting the pump flow rates. At the end of this phase, the entire sand pack was filled with CO_2 foam ready for the oil flood. This was the object of this experiment because, it represents post- fracture clean up during production of hydrocarbon. As the total flow rate during foam flood was 6

ml/min, the oil flood was performed at the same flow rate. The effluent was collected in a burette and the volume of the aqueous phase (1% 2AM or 8:2 2AM: PECNP solution) was noted. The differential pressure across the sand pack was recorded using Lab-View. Reaching the plateau in pressure vs time means we have reached the end of the cleanup process. At this point, the pump was stopped. After oil flood, another brine flood was performed under the same conditions. After that the system was depressurized gradually and cleaned. The fracture clean up experiment was performed in the same setup in which fluid loss experiment was performed, shown in Figure 6.

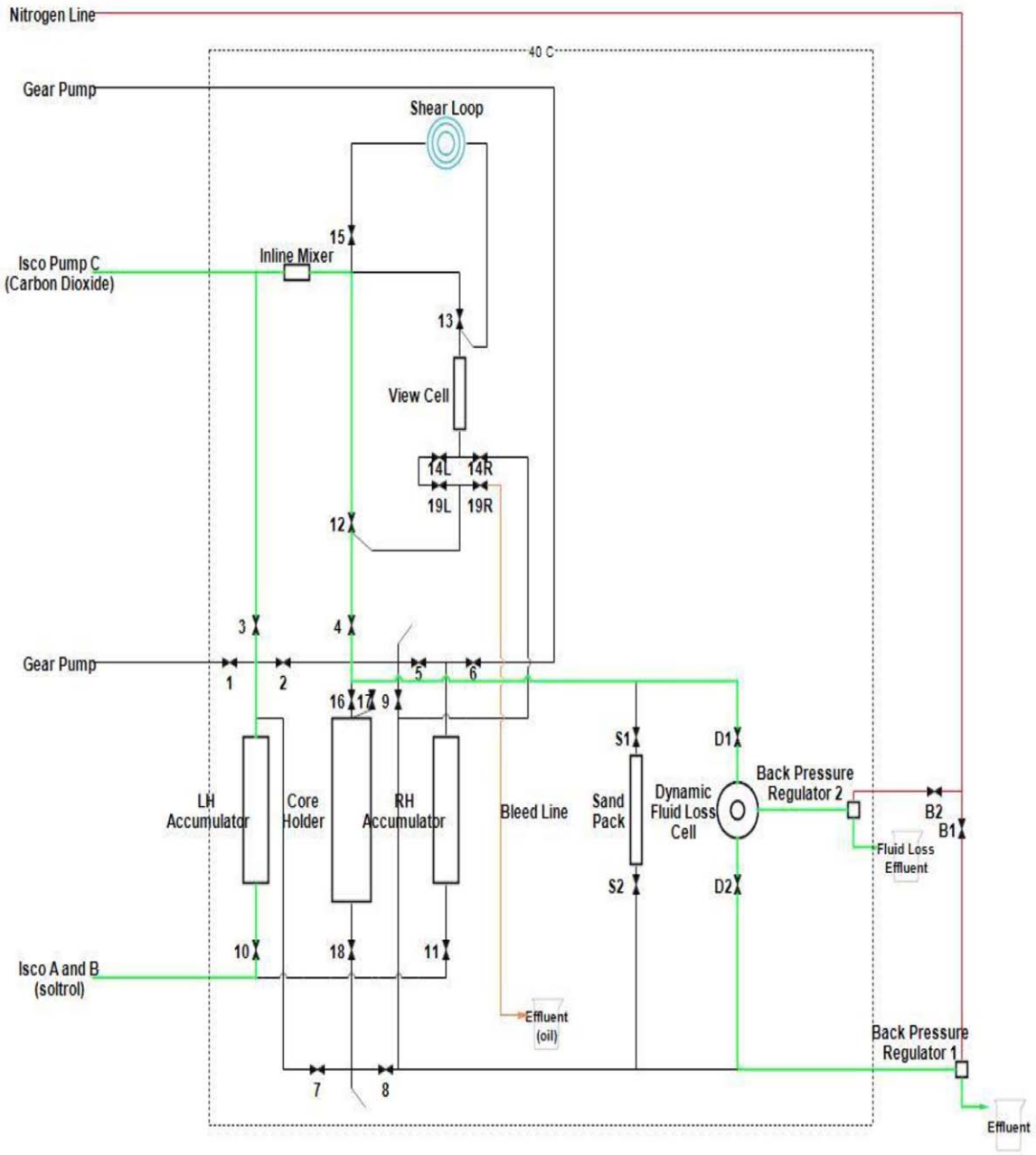

Figure 6—Schematic flow diagram of HPHT CO_2 foam setup, capable of performing fluid loss, clean up, foam stability and core flooding measurements

Results and Discussion

Interfacial Tension Measurements

Tests were performed for both air-aqueous phase and $scCO_2$-aqueous phase systems. Aqueous phase solutions were 2AM-PECNP at ratios of 9:1, 8:2, 7:3 and 6:4, surfactant solution with no PECNP (1 wt% 2AM), brine (2% NaCl) and RO water. The PECNP formulation used was 3:1:0.1 of PEI: DS: 2% NaCl with PEI pH of 8.5. As the measured IFT was dynamic, IFT vs time was plotted.

From Figure 7 and Figure 8 it can be observed that salinity increases IFT, as brine has higher IFT than RO water. Due to preferential positioning of surfactant molecules at the interface, adding surfactants to the brine drastically reduced the IFT. However, adding PECNP reduced the IFT even further, with surfactant-PECNP ratios of 9:1 and 8:2 having the lowest value of IFT. All the systems of $scCO_2$- aqueous phase had lower IFT than air-aqueous phase at 1300 psi and 40°C.

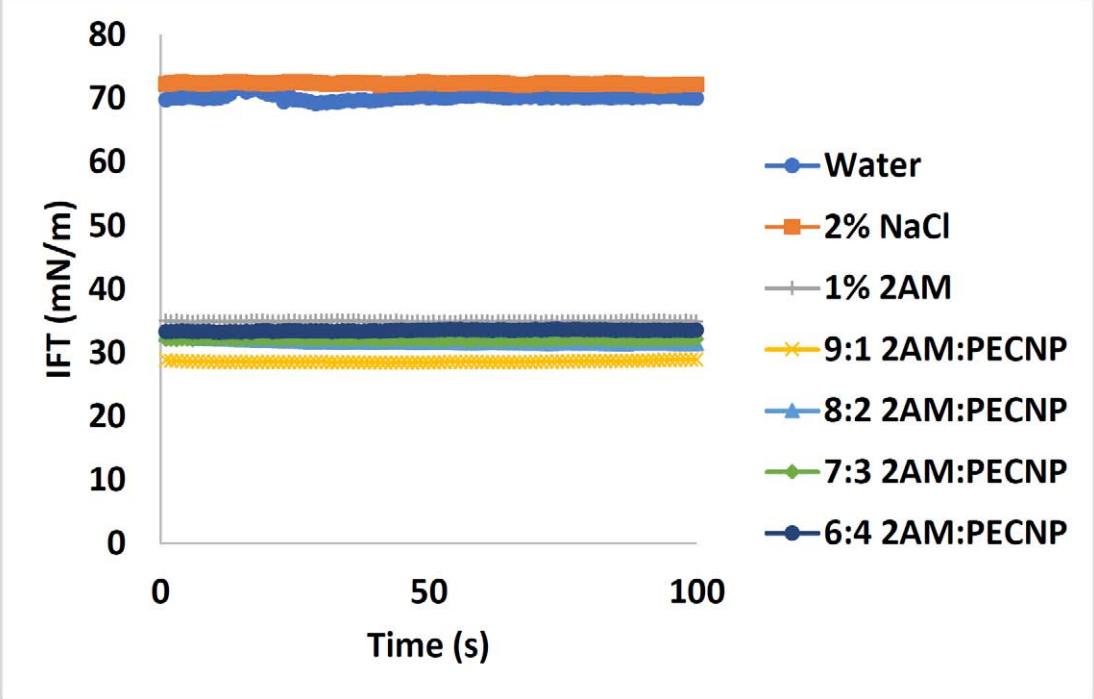

Figure 7—IFT vs time for different surfactant-PECNP system as the aqueous phase and air as the gaseous phase

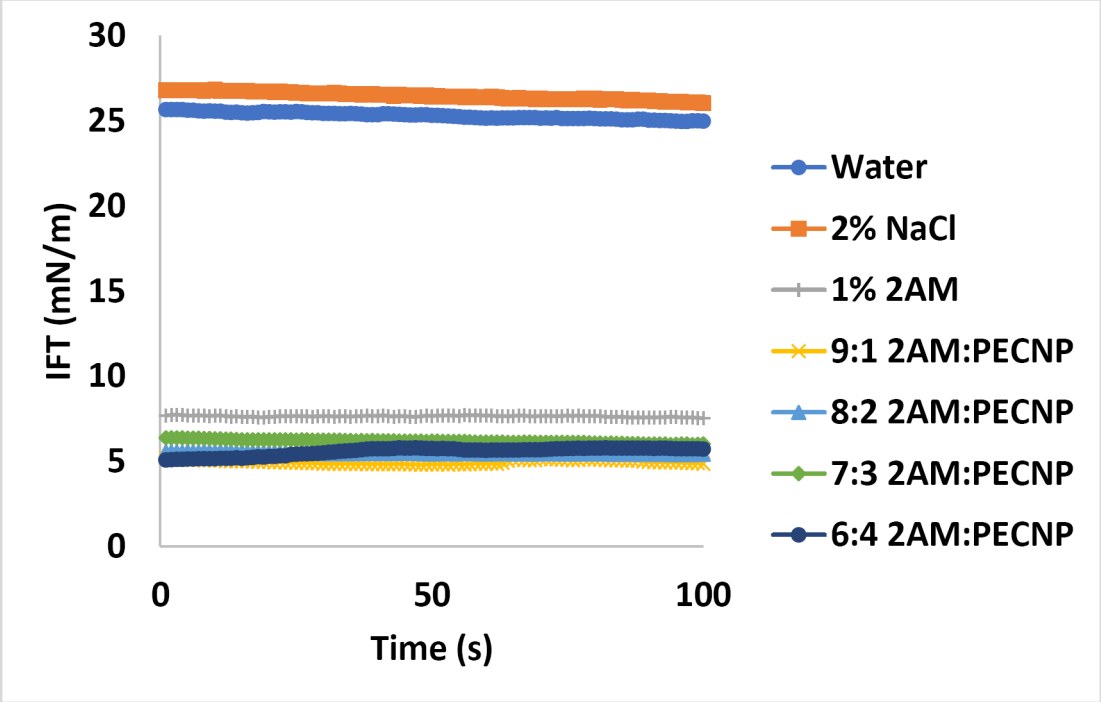

Figure 8—IFT vs time for different surfactant-PECNP systems as the aqueous phase and supercritical CO_2 as the gaseous phase

Porosity and Permeability Measurement of Kentucky Core

Table 1—Porosity of core K8 used for dynamic fluid loss experiments

Kentucky Core- K8	
Pore Volume (cm^3)	1.43
Bulk Volume (cm^3)	11.18
Porosity (%)	12.81

Core flood experiment was conducted with brine (2% NaCl) to measure the permeability of the core. The measurements were performed both before and after the dynamic fluid loss test, and no significant change in core permeability was observed. The flow rate vs pressure drop of the core flood experiments was ploted as shown in Figure 9, slope of this curve was used to calculate the permeability of the core, using Equation 4. The permeability of the Kentucky core used for the dynamic fluid loss experiment was 0.11 mD.

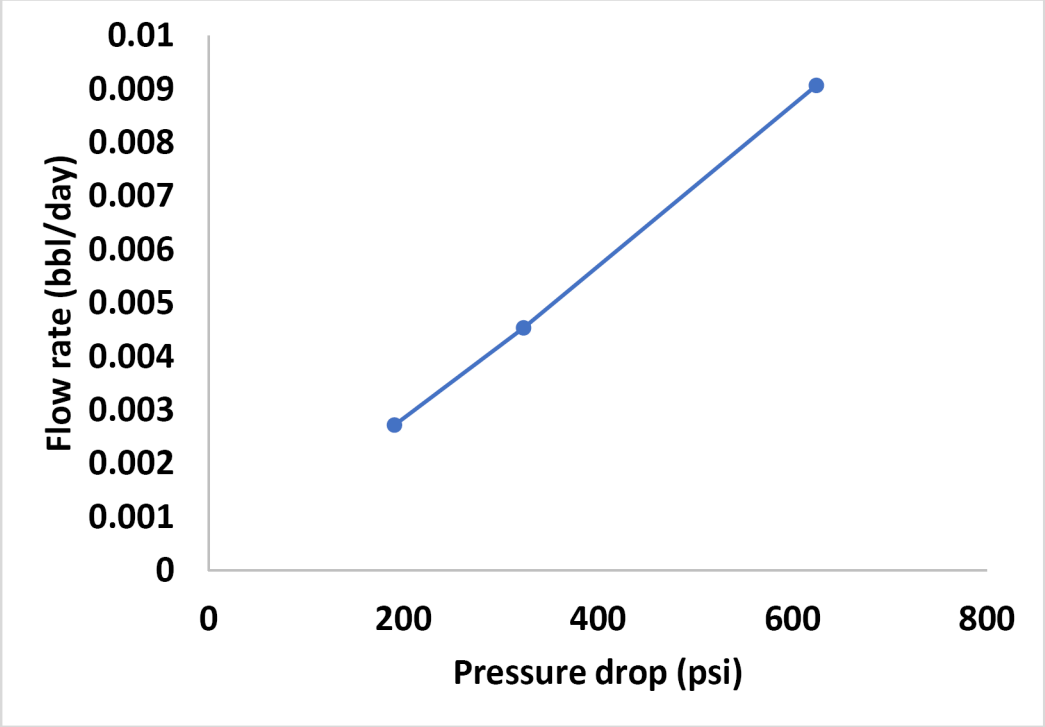

Figure 9—Flow rate vs pressure drop for permeability measurement of Kentucky core

Dynamic Fluid Loss Test

It was found from the rheology and view cell tests that surfactant-PECNP (Anandan et al., 2017) generated CO_2 foam has better rheological properties and stability than foam generated just by surfactant (1% 2AM), and surfactant-PECNP system of 8:2 2AM: PECNP proved to be the most optimal system. In this section, dynamic fluid loss properties of surfactant-PECNP foam are compared with CO2 foam generated just by surfactant (1% 2AM) to decide whether addition of PECNP to surfactant solution reduces the fluid loss.

From Figure 10, it can be observed that the total fluid loss is lower for CO_2 foam generated by optimal surfactant-PECNP ratio of 8:2 compared to foam generated only by surfactant (1 wt% 2AM). This resulted in lesser fluid loss coefficient for CO_2 foam generated by optimal surfactant-PECNP ratio of 8:2 compared to foam generated only by surfactant (1 wt% 2AM), which is shown in Figure 12. Fluid loss coefficient fell by 57%, 10%, 15% and 38% by adding PECNP to surfactant solution for foam qualities of 70%, 80%, 90% and 95% respectively. Nanoparticles formulation enhance the formation resistance to flow which results in effective inhibition of leak-off, thus reducing the likehood of formation damage.

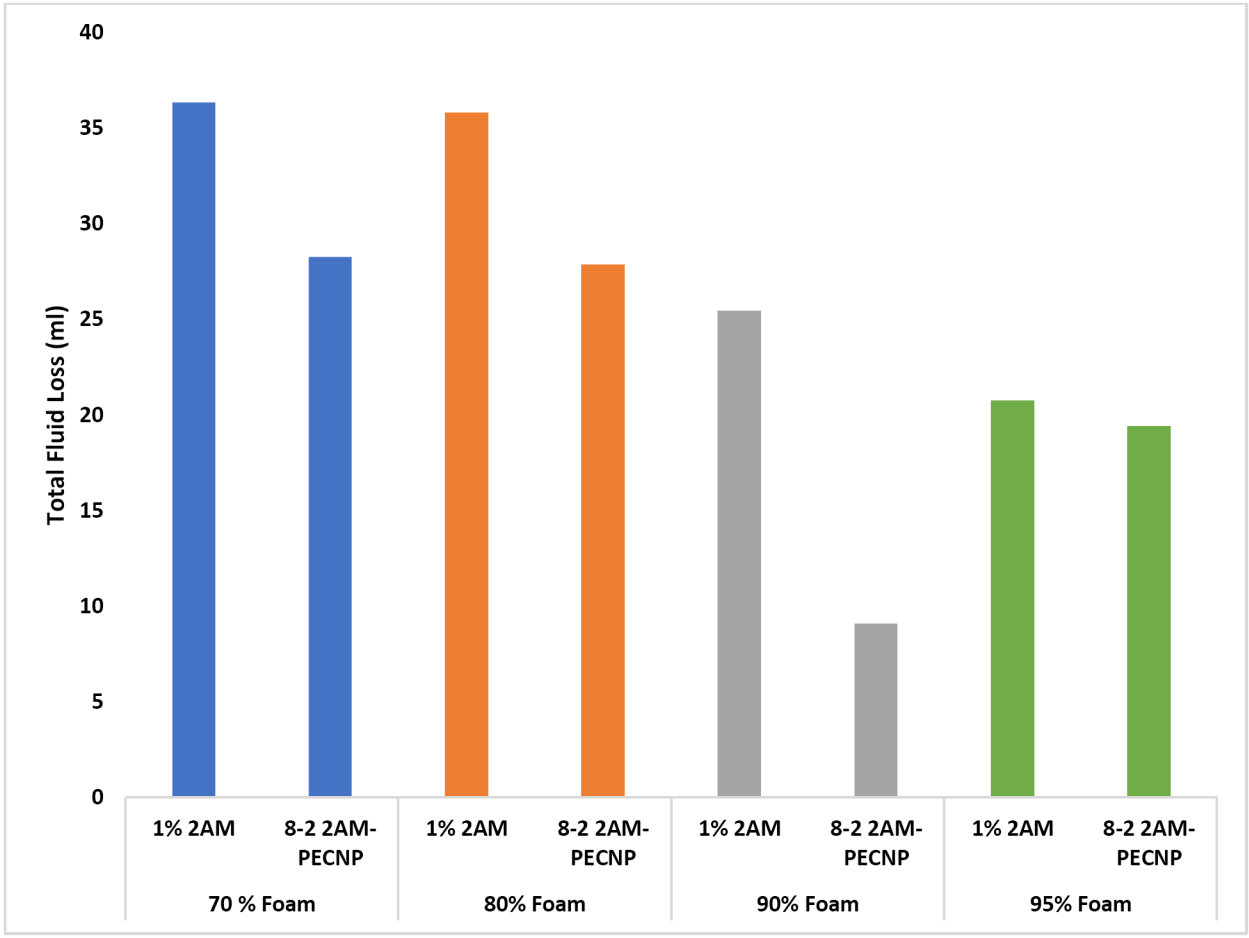

Figure 10—Graph comparing total fluid loss of surfactant and optimal surfactant-PECNP generated CO_2 foam of all the four foam qualities

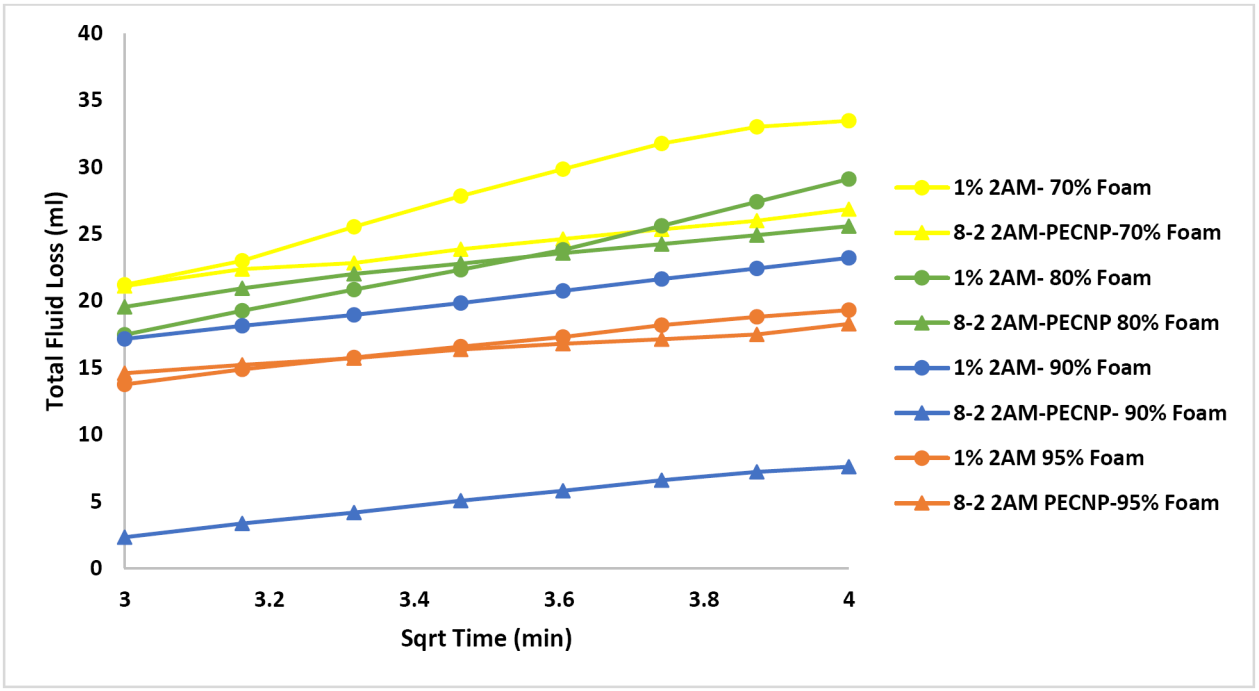

Figure 11—Graph representing the linear part of the total fluid loss vs square root of time curve for surfactant and optimal surfactant-PECNP generated CO_2 foam at various foam qualities

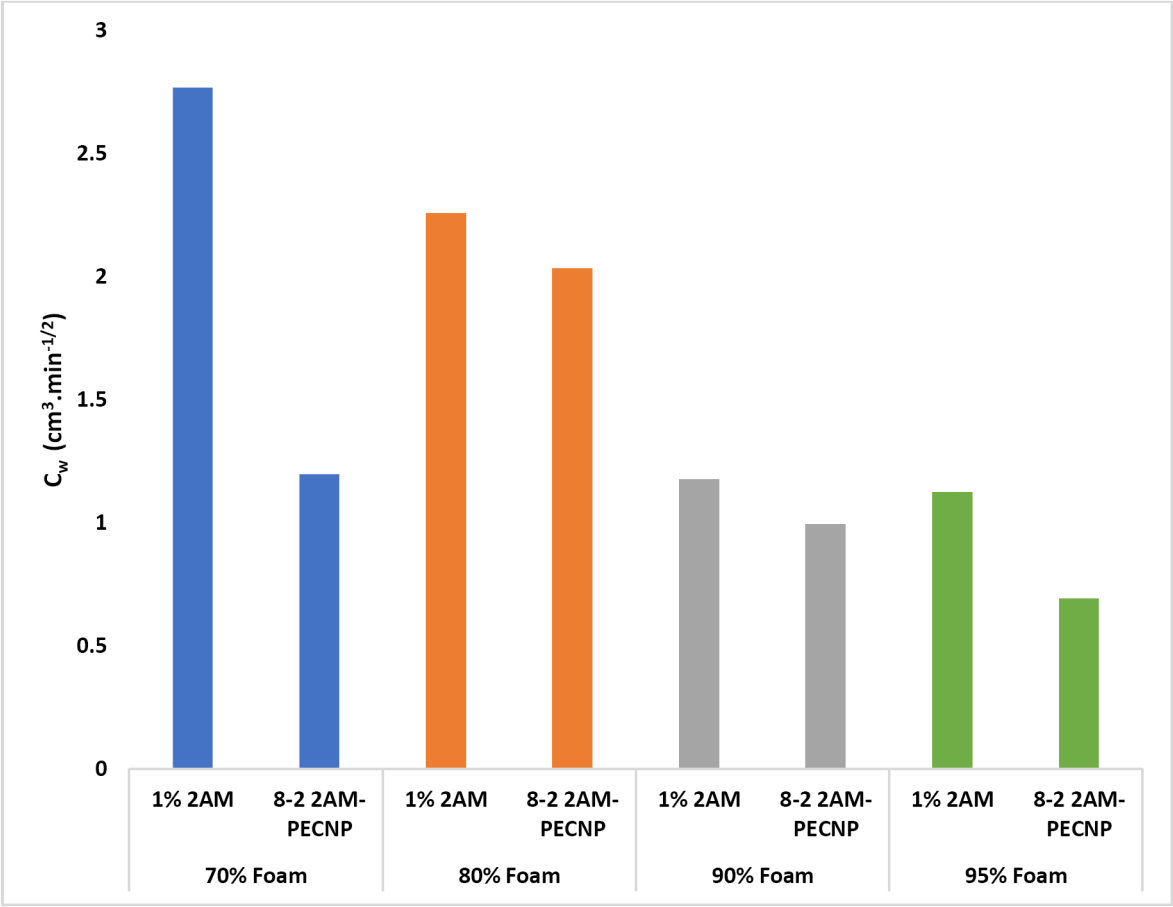

Figure 12—Graph comparing fluid loss coefficient of surfactant and optimal surfactant-PECNP generated CO_2 foam systems for all the four foam qualities

Fracture Cleanup Study

Sand pack tests were performed to analyze the cleanup process of supercritical CO_2 foam as fracturing fluid. Efficiency of cleanup process by CO_2 foam generated by only surfactant (1 wt% 2AM) and the optimal surfactant-PECNP ratio of 8:2 (Anandan et al., 2017) were compared for all four foam ratios of 70%, 80%, 90% and 95%. Pore volume of the sand pack was measured by mass balance and it was determined to be 6.95 cm^3.

Brine Flood

Brine floods were performed at flow rates of 6ml/min, 10 ml/min and 12 ml/min. The pressure drop vs time of the brine flood is shown in Figure 13.

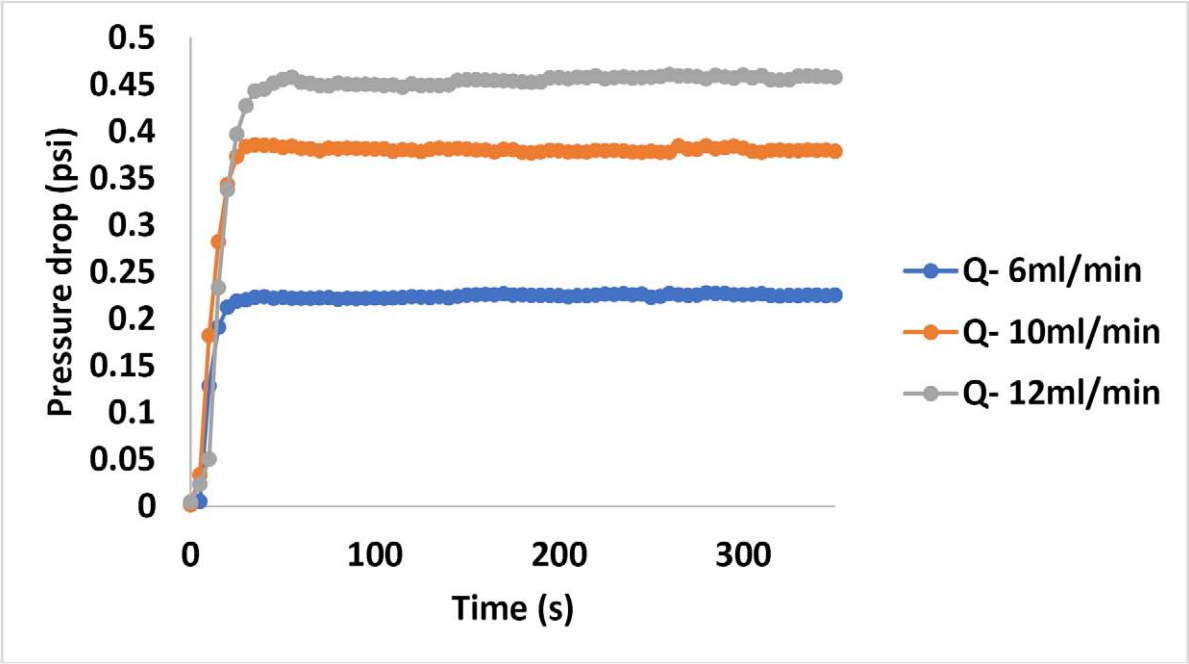

Figure 13—Pressure drop vs time across the sand pack during brine flood at three different flow rates

Foam Flood

Foam flooding was performed after each brine flood. CO_2 foam generated by surfactant and surfactant-PENCP ratio of 8:2 of foam qualities of 70%, 80%, 90% and 95 % were tested. From Figure 14 it can be observed that with increase in foam quality the pressure drop increases, because the viscosity of foam increases with foam quality (Anandan et al., 2017). PECNPs add to the charge of the lamellae and reduce drainage and coalescence resulting in higher pressure drops.

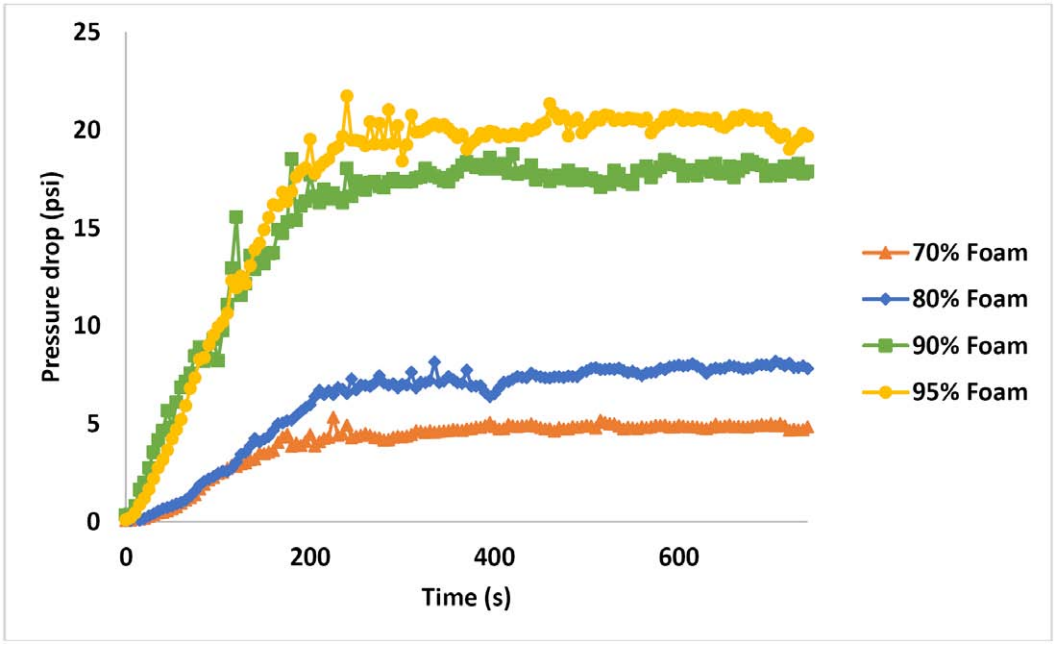

Figure 14—Pressure drop across the sand pack with time for the CO_2 foam generated by most optimal ratio of 2AM-PECNP in each of the four different foam qualities

From Figure 15 to Figure 18, it can be seen that pressure drop for optimized 2AM-PECNP generated foam is higher than foam generated only by surfactant, because addition of PECNP improved the viscosity of foam compared to foam generated just by surfactant (Anandan et al., 2017), as PECNPs add to the charge of the lamellae and reduce drainage and coalesence resulting in improved viscosity which in turn results in higher pressure drops.

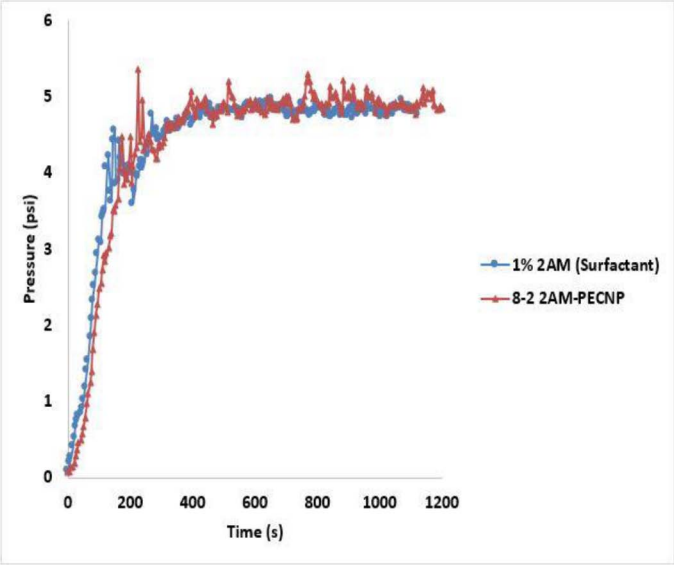

Figure 15—Pressure drop across the sand pack with time for the CO2 foam generated by surfactant and 8:2 ratio of 2AM-PECNP with foam quality of 70%

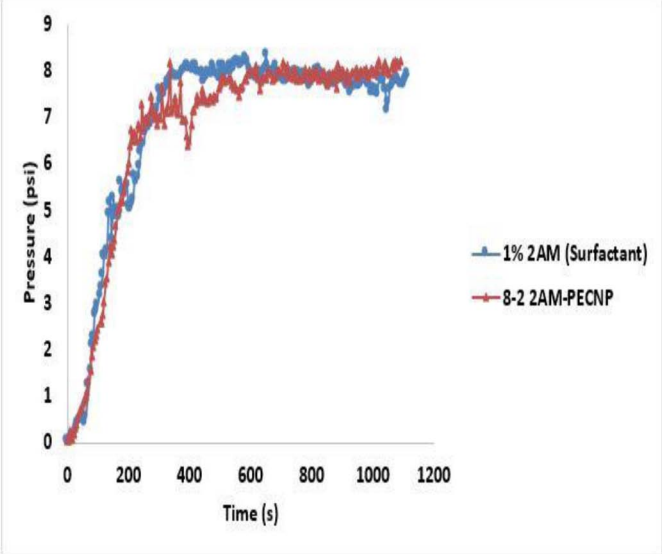

Figure 16—Pressure drop across the sand pack with time for the CO2 foam generated by surfactant and 8:2 ratio of 2AM-PECNP with foam quality of 80%

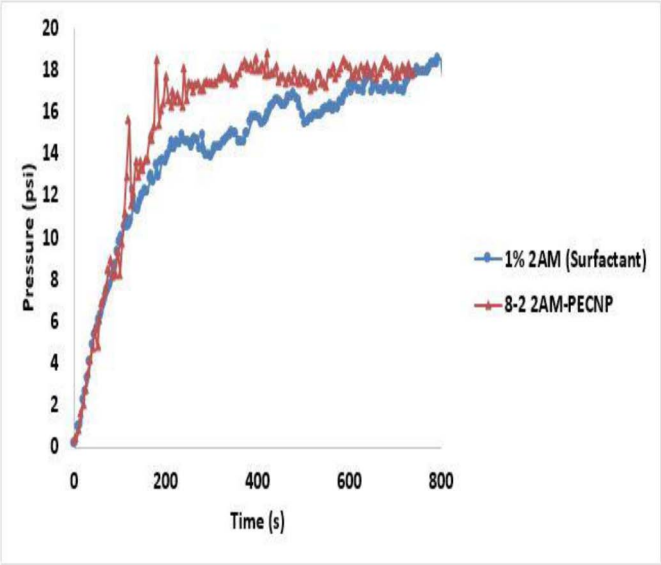

Figure 17—Pressure drop across the sand pack with time for the CO2 foam generated by surfactant and 8:2 ratio of 2AM-PECNP with foam quality of 90%

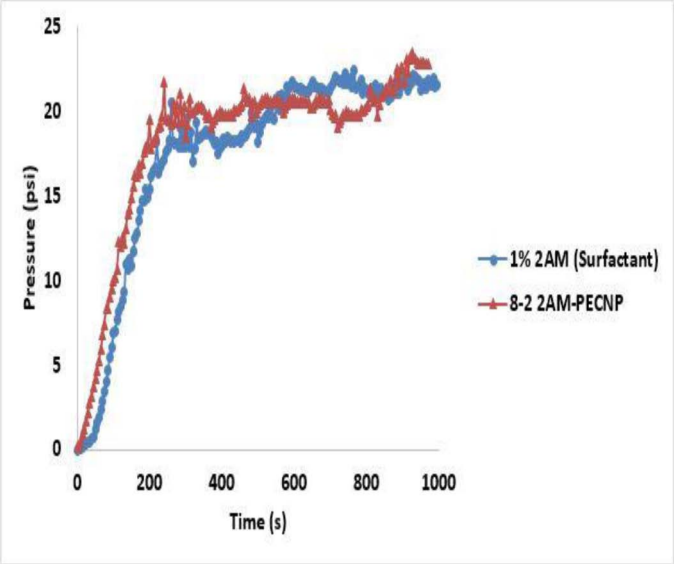

Figure 18—Pressure drop across the sand pack with time for the CO2 foam generated by surfactant and 8:2 ratio of 2AM-PECNP with foam quality of 95%

Oil Flood after Foam Flood

After the foam flood, the sand pack with proppants was filled with foam and crude oil was injected. Injection of crude oil into the sand pack represents the post fracture clean up due to production of hydrocarbon. The aqueous phase in the effluent was collected in a burette during the oil flood. Clean up of the foam generated by surfactant and 8:2 ratio of surfactant-PECNP was compared with cleanup of just brine (2 wt% NaCl).

Figures 19 to 22 show, that pressure drop for the cleanup of brine is slightly higher than CO_2 foam. Imbibition of oil into the foam lamellae causes contraction and expansion of lamellae (Marangoni flow) and, will result in thinning of the pseudo-emulsion film (Talebian et al., 2013). This causes foam to destabilize and break in the presence of crude oil (Schramm, 1994).

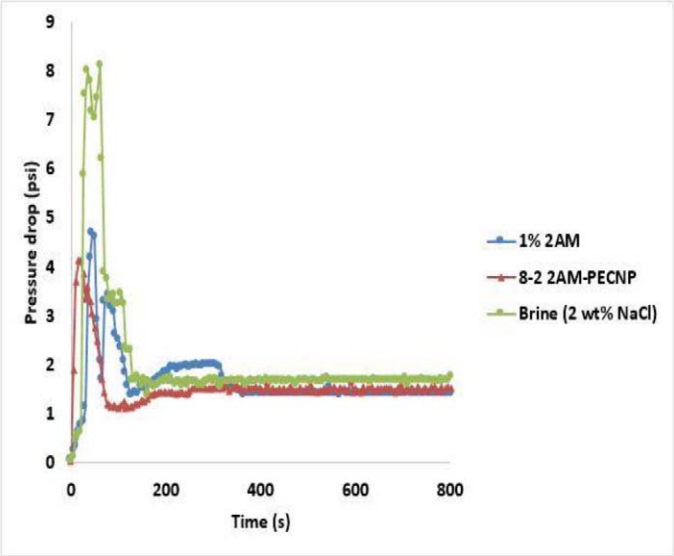

Figure 19—Pressure drop across the sand pack with time for the cleanup of CO2 foam generated by surfactant and 8:2 ratio of 2AM-PECNP with foam quality of 80 % during oil flood

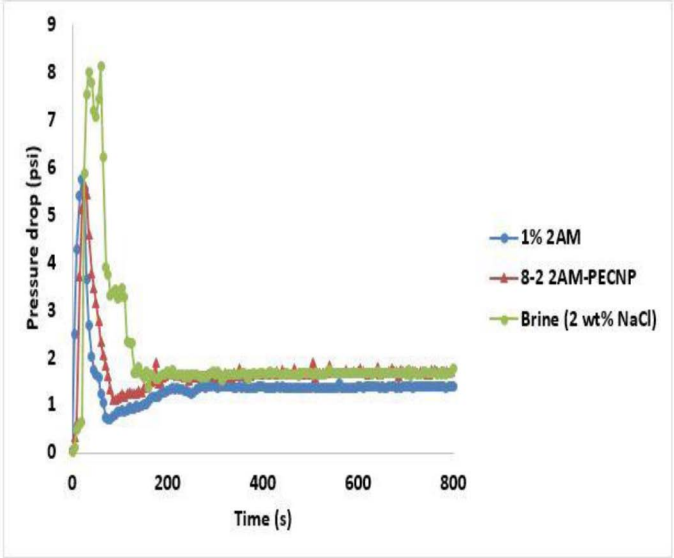

Figure 20—Pressure drop across the sand pack with time for the cleanup of CO2 foam generated by surfactant and 8:2 ratio of 2AM-PECNP with foam quality of 80 % during oil flood

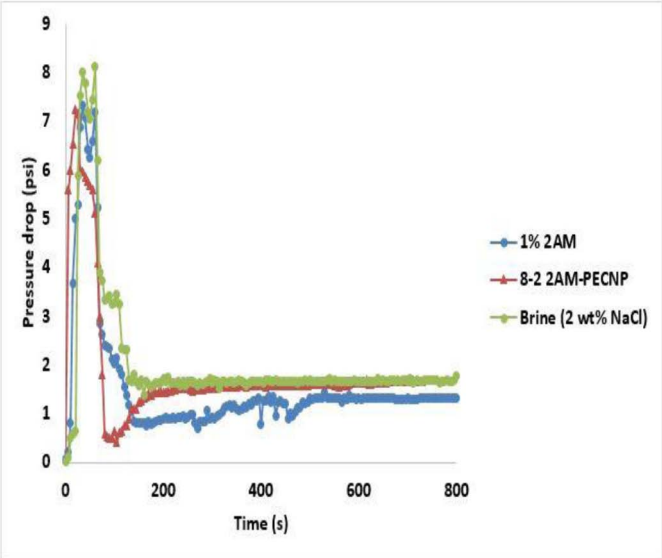

Figure 21—Pressure drop across the sand pack with time for the cleanup of CO2 foam generated by surfactant and 8:2 ratio of 2AM-PECNP with foam quality of 90 % during oil flood

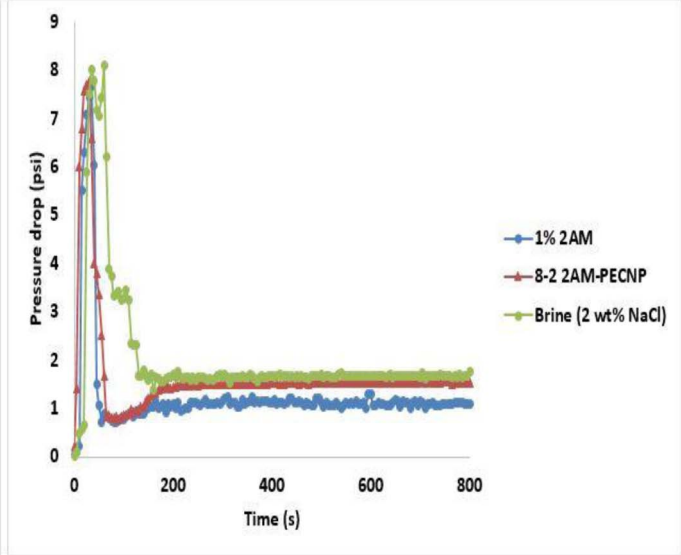

Figure 22—Pressure drop across the sand pack with time for the cleanup of CO2 foam generated by surfactant and 8:2 ratio of 2AM-PECNP with foam quality of 95 % during oil flood

Aqueous Phase Recovery after Oil Flood:

The effluent from the oil flood was collected in a burette and the volume of the recovered aqueous phase was measured. Maximum volume (V_{max}) of aqueous phase after the foam flood in the sand pack can be calculated using Equation 6, given below,

$$V_{max}\,(ml) = (1 - (\text{Foam Quality}\ (\%)/100)) * V_p \qquad \text{Equation 6}$$

Surfactant recovery can be calculated using Equation 7 given below,

$$\text{Surfactant Recovery}\ (\%) = (V/V_{max}) * 100 \qquad \text{Equation 7}$$

where,

V : Volume of aqueous phase (surfactant or surfactant-PECNP solution) collected in burette after the oil flood (ml)

Figure 23 shows aqueous phase recovery after oil flood. The aqueous phase recovery after oil flood for CO_2 foam generated by the optimal surfactant-PECNP ratio is greater than foam generated by surfactant alone. This means that flow back of CO_2 foam generated by the surfactant-PECNP is better than foam generated only by surfactant.

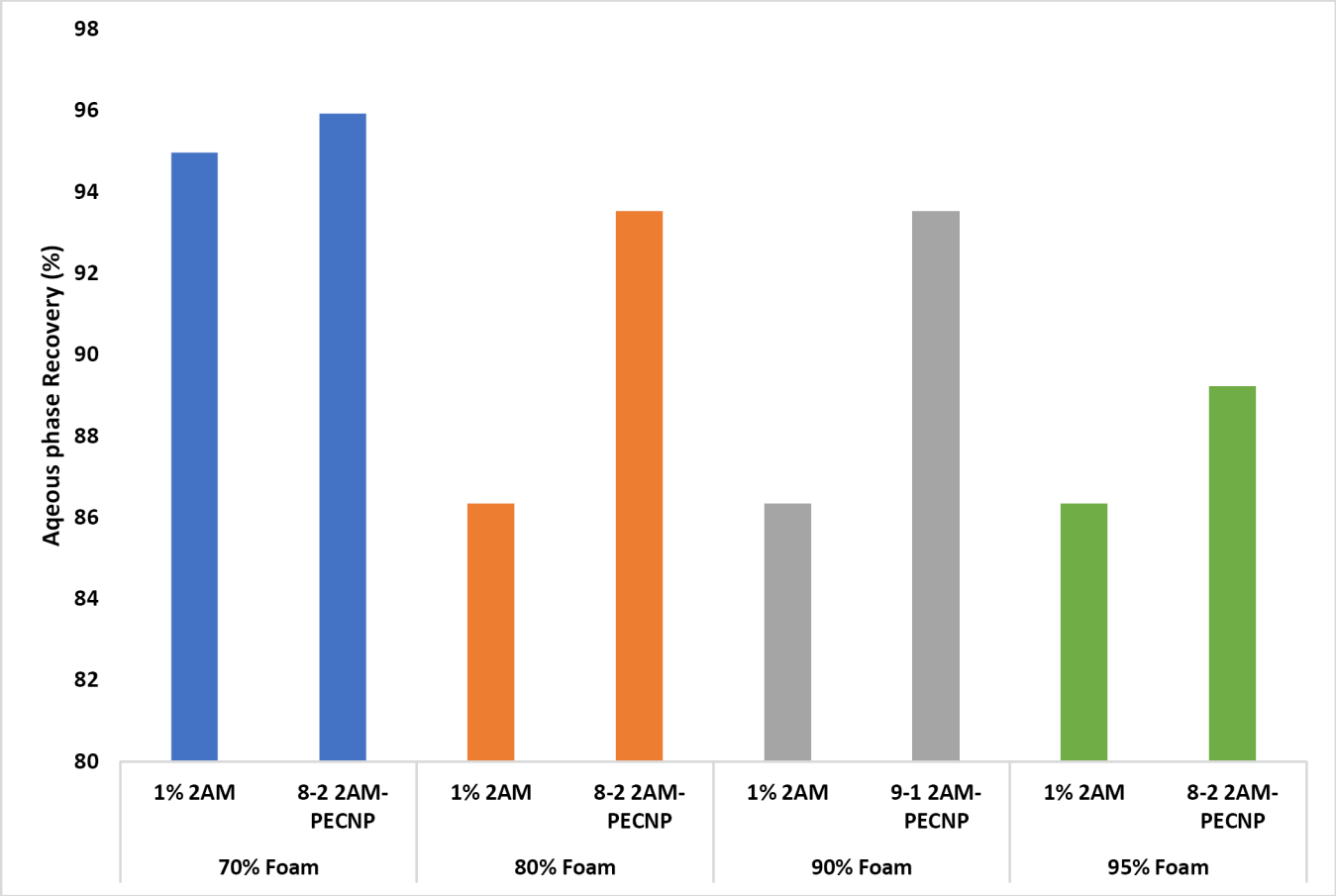

Figure 23—Comparison of aqueous phase recovery (%) after the oil flood between cleanups of CO_2 foam generated by surfactant and most optimal surfactant-PECNP system at all the four different foam qualities

Conclusions

Addition of PECNP to the surfactant solution generated foam with enhanced foam stability and viscosity (Anandan et al., 2017) compared to foam generated just by surfactant. In the previous study (Anandan et al., 2017), PECNP formulation was optimized based on minimizing particle size, increasing the zeta potential, viscosity and stability; the optimal formulation was determined to be the one with 8:2 ratio of 2AM-PECNP. In this study, dynamic fluid loss and post fracture clean up efficiency of $scCO_2$ foam stabilized by addition of optimized PECNP as fracturing fluid was investigated.

1. Interfacial Tension Measurements: Influence of salinity, addition of PECNP to surfactant solution on interfacial tension between air-aqueous phase and $scCO_2$-aqueous phase were studied. The interfacial tension results were similar in both air-aqueous phase and $scCO_2$-aqueous phase systems. Addition of surfactant to brine solution significantly reduced the IFT, but the IFT was further reduced with addition of PECNP.
2. Dynamic Fluid Loss Tests: Addition of optimized PECNP formulation to surfactant solution decreased the fluid loss in all four foam qualities studied, this resulted in lower fluid loss coefficient for foam generated using surfactant-PECNP solution than for foam generated using only surfactant solution.

Fluid loss coefficient fell by 57%, 10%, 15% and 38% by adding PECNP to surfactant solution for foam qualities of 70%, 80%, 90% and 95% respectively.

3. Clean-up Tests: Sand pack tests were performed to study the post fracture clean-up of $scCO_2$ foam and influence of addition of PECNP to surfactant solution. Clean-up of foam was compared with brine (2% NaCl). Based on the pressure drop across the sand pack during the clean-up experiment and volume of aqueous phase collected after injection of crude oil, $scCO_2$ foam as fracturing fluid showed better clean up compared to brine. In fact, foam (both with and without PECNP) showed 91% average phase recovery of fracturing fluid after the oil flood. Moreover, the clean-up further improved by adding optimized PECNP formulation to surfactant solution.

Acknowledgements

This project is partially funded by a National Science Foundation EPSCoR Research Infrastructure Improvement Program: Track −2 Focused EPSCoR Collaboration award (OIA- 1632892). The authors would like to extend their appreciation to Harcos Chemicals Inc. for supporting this project with a supply of their surfactants. We would like to thank Zach Kessler and Scott Ramskill from the Chemical and Petroleum Engineering department and Tertiary Oil Recovery Program (TORP) at the University of Kansas for their help and support.

Nomenclature

μ : Viscosity, cP
k : Permeability (mD)
ΔP : Differential pressure (psi)
Q : Flow rate (ml/min)
L : Length of the core (cm)
V_L : Total fluid loss (cm^3)
C_w : Fluid loss coefficient
V_s : Spurt fluid loss (cm^3)
V : Volume (cm^3)
T : Temperature (°C)
n : number of moles
R : Ideal gas constant

References

1) Ahmed, U, and Meehan, N., (2016). *Unconventional Oil and Gas Resources: Exploitation and Development*. Taylor Francis Group, Baker Hughes, https://www.crcpress.com/Unconventional-Oil-and-Gas-Resources-Exploitation-and-Development/AhmedMeehan/p/book/9781498759403.
2) Al-Dhamen, M, and Soriano, E., (2015). Increased Well Productivity from the Use of Carbon Dioxide to Foam Fracturing Fluids During a Refracturing Treatment in Saudi Arabia. SPE Latin American and Caribbean Petroleum Engineering Conference, Quito, Ecuador, 18-20 November. SPE-177112-MS: *Society of Petroleum Engineers*.
3) Amstrong, K. (1996). Advanced Fracturing Fluid Improve Well Economics. *Oil Field Review*.
4) Anandan, R., Johnson, S., and Barati, R., (2017). Polyelectrolyte Complex Stabilized CO2 Foam Systems for Hydraulic Fracturing Application. SPE Liquids-Rich Basins Conference- North America held in Midland, TX, USA, 13-14 September 2017. SPE.
5) Barati. (2010). *Fracturing Fluid Cleanp by Controlled Release of Enzymes from Polyelectrolyte Complex nanoparticles*. University of Kansas, Lawrence.

6) Barati, R. et al. (2009). Fracture Impact of Yield Stress and Fracture-Face Damage on Production with a Three Phase 2D Model. *SPE Production and Operations Journal*, **24**(2): 336–345.
7) Barati., R, and Liang, J.T., (2014). A Review of the Polymeric Fracturing Fluid Systems Used for Hydraulic Fracturing of Oil and Gas Wells. *Journal of Applied Polymer Science*.
8) Blauer, R. E. and Kohlhaas, C, A., (1974). Formation Fracturing with Foam. Fall Meeting of the Society of Petroleum Engineers of AIME, 6-9 October, Houston, Texas. https://doi.org/10.2118/5003-MS. SPE.
9) Burke, L. H. and Nevison, G. W. (2011). Improved Hydraulic Fracture Performance with Energized Fluids: A Montney Example. *Recovery-2011 CSPG CSEG CWLS Convention*.
10) Cawiezel, K. E. and Niles, T, D., (1987). Rheological Properties of Foam Fracturing Fluids Under Downhole Conditions. SPE Production Operations Symposium, 8-10 March, Oklahoma City, Oklahoma. SPE.
11) Chancellor, R., (1977). Mesaverde hydraulic fracture stimulation, northern Piceance Basin – progress report,. *Exploration Frontiers of the Central and Southern Rockies (Denver: Rocky Mountain Association of Geologists, 1977)* 285–291.
12) Charlez, P. A., (1997). *Rock Mechanics: Petroleum Applications*. Paris: Editions Technip. p. 239. ISBN 9782710805861. Retrieved 2012-05-14.
13) Detlef, M., (1989). *Hydraulic Proppant Fracturing and Gravel Packing*. Elsevier. pp. 173–174; 202. ISBN 9780444873521.
14) Economides, M. J and Nolte, K.G., (2000). *Reservoir Stimulation*, third edition. Wiley, New York and Chichester.
15) Enick, R. M. and Olsen, D, K., (2012). Mobility and Conformance Control for Carbon Dioxide Enhanced Oil Recovery (CO2-EOR) via Thickners, Foams, and Gels- A Detailed Literature Review of 40 years of Research. *U.S. Department of Energy*.
16) EPA. (2011). *Draft Plan to Study the Potential Impacts of Hydraulic Fracturing on Drinking Water Resources*. https://yosemite.epa.gov/sab/sabproduct.nsf/0/D3483AB445AE61418525775900603E79/$File/Draft+Plan+to+Study+the+Potential+Impacts+of+Hydraulic+Fracturing+on+Drinking+Water+Resources-February+2011.pdf.
17) Fast, C. R. et al., (1977). "The application of massive hydraulic fracturing to the tight Muddy 'J' Formation, Wattenberg Field, Colorado. *Exploration Frontiers of the Central and Southern Rockies (Denver: Rocky Mountain Association of Geologists, 1977)* 293–300.
18) Friehauf, K. E., (2009). Fluid Selection for Energized Hydraulic Fractures. SPE Annual Technical Conference and Exhibition, 4-7 October, New Orleans, Louisiana. SPE-124361-MS. https://doi.org/10.2118/124361-MS.
19) Friehauf, K. E. and Sharma, M., (2009). Application of a New Compositional Model for Hydraulic Fracturing With Energized Fluids: A South Texas Case Study. SPE Hydraulic Fracturing Technology Conference, 19-21 January, The Woodlands, Texas. SPE.
20) Gandossi, L and Von Estorff, U., (2013). An overview of hydraulic fracturing and other formation stimulation technologies for shale gas production. *EUR 26347: Joint Research Centre Science Hub, European Commision*.
21) Grundmann, S, R. and Lord, D, L. (1983). Foam Stimulation. *Journal of Petroleum Technology SPE-9754-PA*.
22) Harris, P. C. (1988). Fracturing-Fluid Additives. *Journal of Petroleum Technology, vol. SPE Distinguished Author Series*,.
23) He, K. et al. (2015). Minimizing Surfactant Adsorption Using Polyelectrolyte Based Sacrificial Agent: a Way to Optimize Surfactant Performance in Unconventional Formations. SPE

International Symposium on Oilfield Chemistry, 13-15 April, The Woodlands, Texas, USA. SPE-173750-MS. https://doi.org/10.2118/173750-MS.

24) Hunter, R.J., (1988). *Zeta Potential in Colloid Science: Principles and Application*. San Diego, California.: ACADEMIC PRESS INC.
25) Kalyanaraman, N. et al., (2015). Stability Improvement of CO2 Foam for Enhanced Oil Recovery Applications Using Polyelectrolytes and Polyelectrolyte Complex Nanoparticle. Presented at SPE Asia Pacific Enhanced oil Recovery Conference, Kuala Lumpur, Malaysia, 11-13 August 2015, SPE-174650-MS.
26) Klitzing, R.V., et al (1997). Forces in foam films containing polyelectrolyte and surfactant. *Science Direct*. https://doi.org/10.1016/S0927-7757(98)00307-0.
27) Kohshour, I. O. et al., (2016). Examination of Water Management Challenges and Solutions in Resource Development- Could Waterless Fracturing Techologies Work?. Unconventional Resources Technology Conference held in San Antonio, Texas, USA, 1-3 August 2016. URTeC: 2461040.
28) Kristen, N. and Klitzing, R, V., (2010). Effect of polyelectrolyte/surfactant combinations on the stability. *Soft Matter, Royal Society of Chemistry* DOI: 10.1039/b917297a.
29) Linde. (2013). *Benefits of Energized Solutions in Fracturing*. Murray Hill, New Jersey: Linde North America, Inc.
30) Makhanov, K. et al., (2012). An Experimental Study of Spontaneous Imbibition in Horn River Shales. SPE Canadian Unconventional Resources Conference, 30 October-1 November, Calgary, Alberta, Canada. SPE.
31) Moayedi, H. et al., (2011). Zeta potential of Organic soil in Presence of Calcium Chloride, Cement and Polyvinyl Alcohol. *International Journal of ELECTROCHEMICAL SCIENCE*; http://www.electrochemsci.org/papers/vol6/6104493.pdf.
32) Montgomery, C. (2013). *Fracturing Fluids. Free Article*.
33) Nazari, N., Tsau, J, S., and Barati, R. CO2 Foam Stability Improvement Using Polyelectrolyte Complex Nanoparticles Prepared in Produced Water. *Energies* **10**, 516 (2017).
34) Nguyen, P. et al., (2014). Nanoparticle Stabilized CO2 in Water Foam for Mobility Control in Enhanced Oil Recovery via Microfluidic Method. SPE Heavy Oil Conference-Canada, 10-12 June, Calgary, Alberta, Canada. SPE-170167-MS. SPE.
35) Osiptsov, A.A., (2017). Fluid Mechanics of Hydraulic Fracturing: a Review. *J. Pet. Sci. Eng.* **156**, 513–535.
36) Penny, G. S et al., (2006). Field Study of Completion Fluids to Enhance Gas Production in the Barnett Shale. SPE Gas Technology Symposium, 15-17 May, Calgary, Alberta, Canada. SPE.
37) Perry, R. H., (1997). *Perry's Chemical Engineering Handbook. Table 2-167*. Seventh Edition. Mcgraw Hill. ISBN 0-07-049841-5.
38) Reidenbach, V. G. et al., (1986). Rheological Study of Foam Fracturing Fluids using Nitrogen and Carbon Dioxide. *SPE Prod Eng*, January, 31–41. SPE 12026-PA.
39) Ribeiro, L. H. and Sharma, M., (2013). Fluid Selection for Energized Fracture Treatments. SPE Hydraulic Fracturing Technology Conference. The Woodlands, Texas, USA.
40) Samuel, M. M. et al., (1999). Polymer free fluid for fracturing Application. *Paper SPE 59478. Drilling and Completion Journal*.
41) Schramm, L. L. (1994). *FOAMS, Fundamentals and Applications in the Petroleum Industry*. Washington D.C:: Advances in Chemistry Series.
42) Sharma, M. and Agrawal, S., (2013, September 26, 2013). Impact of Liquid Loading in Hydraulic Fractures on Well Productivity. Society of Petroleum Engineers. SPE Hydraulic

Fracturing Technology Conference, 4-6 February, The Woodlands, Texas, USA. SPE-163837-MS. SPE.

43) Talebian, S. H. et al., (2013). Foam assissted CO2- EOR; Concepts, Challenges and Applications. SPE EOR conference. Kuala Lumpur, Malaysia.

44) Veisi, M. et al., (2018). Application of Polyelectrolyte Complex Nanoparticles to Increase the Lifetime of Poly Vinyl Sulfonate Scale Inhibitor. SPE International Conference and Exhibition on Formation Damage Control, 7-9 February 2018, Lafayette, Louisiana, USA.

45) Yang, W. et al., (2017). Foams Stabilized by in-situ Modified Nanoparticle and Anionic Surfactants for Enhanced Oil Recovery. *Energy and Fuels* **31**, 4721–4730.

46) Yost, A.B., (1994). Analysis of Production Response to CO_2/Sand Fracturing: A Case Study. SPE Eastern Regional Meeting, 8-10 November, Charleston, West Virginia. SPE-29191-MS. https://doi.org/10.2118/29191-MS.

47) Yu, J. et al., (2012). Foam Mobility Control for Nanoparticle-Stabilized Supercritical CO2 Foam. SPE Improved Oil Recovery Symposium, 14-18 April, Tulsa, Oklahoma, USA. SPE-153336-MS. https://doi.org/10.2118/153336-MS.